

THREE-DIMENSIONAL MODELLING OF NON-NEWTONIAN FLUID FLOW IN A COAT-HANGER DIE

Su Yeon Na and Do Hyun Kim[†]

Department of Chemical Engineering, Korea Advanced Institute of Science and Technology,
373-1 Kusong-dong, Yusong-gu, Taejon 305-701

(Received 17 August 1994 • accepted 21 December 1994)

Abstract—The three-dimensional model of isothermal flow of power-law fluid in a coat-hanger die has been developed using finite element method. The shape of coat-hanger die used in the present model was determined according to the previous analytical design equation which is based on one-dimensional flow model in the manifold and the slot. Because uniform flow rate across the die outlet is most important to achieve uniform thickness of extruded polymer sheet or film, flow rate distribution is mainly examined to determine the valid process condition for the design equation as the design parameters are changed. The effects of fluid property in terms of power-law index and process parameters not considered in one-dimensional design equation such as die inlet size and the presence of land were analyzed. Results show that the manifold angle is the most influencing design parameter on flow rate distribution. When the material of different power-law index from design value is processed, the change of power-law index affects the uniformity of flow rate appreciably.

Key words: Coat-Hanger Die, 3-D Model, Simulation, FEM, Power-Law Fluid

INTRODUCTION

The coat-hanger dies are widely used in the polymer processings for the production of sheets and films. Both the geometrical and material quality of the products is governed by the uniformity of flow rate and residence time distributions. To satisfy these conditions, the optimal design of the coat-hanger dies has been a major research interest for many years.

The first attempt at the optimal sheet die was made through the T-dies with the horizontal manifold [Carley, 1954, 1956; Matsubara, 1980a; McKelvey and Ito, 1971; Pearson, 1964]. Many of these works on the T-dies revealed the necessity of the more versatile dies with the tapered manifold of varying cross-sectional area and the tapered slot section because T-dies were not able to provide sufficient flow uniformity for the production of the wide sheets and films. The design problem of the coat-hanger dies was studied by many investigators [Klein and Klein, 1973; Lee and Liu, 1989; Liu et al., 1988; Matsubara, 1979, 1980b, 1983; Procter, 1972; Tadmor and Gogos, 1979; Winter and Fritz, 1986]. The designs of T-die and coat-hanger die were mainly carried out by analytic method under the assumptions that both the flows in the manifold and the slot are fully-developed in the machine direction and have no interactions, using power-law fluid for the polymer melts. Most of these analyses can be termed as the one-dimensional models of the flow in the manifold and the slot, which neglect the interaction between two flows. Although the derivation is straightforward, the analytic approaches are physically too restrictive in assumptions and cannot provide sufficient information on the flow fields. In order to get a detailed and realistic description on the flow fields in the dies, numerical analysis based on model of higher dimension should be conducted.

Most of the numerical approaches were carried out based on

the two-dimensional flow model and the lubrication approximation [Arpin et al., 1992; Booy, 1982; Gutfinger et al., 1975; Tadmor et al., 1974; Vergnes et al., 1984; Vrahopoulou, 1991]. The two-dimensional analysis need relatively lower load of computation and can be applied easily. But application of the two-dimensional analysis to coat-hanger dies is not satisfactory because two-dimensional analysis cannot take account of the geometrical features of the die inlet and the manifold where distribution of the flows—the major function of the coat-hanger dies—is accomplished. Thus, the flows in the coat-hanger dies should be modelled as three-dimensional for more realistic interpretation.

Among the several numerical analysis techniques for the fluid flow simulation, finite element method is considered as the powerful tool by the ability to easily deal with the complex geometry and boundary conditions. Recently there have been efforts to apply three-dimensional finite element method to the flow in the coat-hanger die by Wang [1991a, b] and fish-tail die by Huang et al. [1993]. In these works several points are noted which can degrade the accuracy of the results. They applied twenty-node brick finite element that has been proved to be inadequate for the solution of Navier-Stokes equation [Fortin, 1981]. Boundary conditions are unphysical at the die wall and exit. Also, they used elements of too large aspect ratio in slot region. They did not consider the design problem of the coat-hanger die and did not investigate the effects of the design parameters on the die performance thoroughly.

In this study, flow analysis has been conducted to examine the validity of the die design. Model of the die for the analysis was determined using the analytical design equation previously developed through one-dimensional analysis. Among several design equations, Liu et al.'s result [1988] was selected because their approach can be applied to the manifold of various cross-sectional shape while most of the other works on the coat-hanger die design assumed circular cross-section. For the numerical sim-

[†]To whom all correspondences should be addressed.

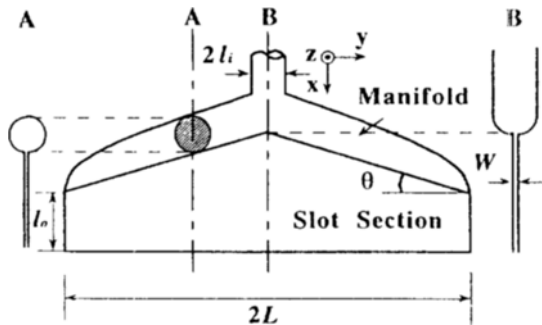


Fig. 1. Geometry of linearly tapered coat-hanger die.

ulation of the polymer flows in the coat-hanger die, the three-dimensional finite element code was developed based on mathematical model. By the results of flow rate distribution calculated from numerical simulation, the one-dimensional design equation was examined to what degree it achieves the design objectives and under what process condition it can be applied safely. This study may provide the basic results concerning the coat-hanger die design in various situations.

MATHEMATICAL FORMULATION

1. Die Design

Model of the coat-hanger die used in this study was designed according to the design equation developed by Liu et al. [1988]. The schematic of the linearly tapered coat-hanger die with the circular manifold is given in Fig. 1. They derived the design equation for the linearly tapered coat-hanger die with the manifold of various cross-sectional shape to obtain uniform flow rate distribution at the die exit in the transverse direction. Polymer melt flow is assumed to be laminar, isothermal, and incompressible. The non-Newtonian behavior of the polymer melt is considered by the power-law model because the material of interest such as LDPE, PMMA, ABS follows this model in wide range of shear rate. To allow the analytic derivation, flows in the manifold and the slot were assumed to be one-dimensional in the main flow direction and to have no interactions each other. They accounted for non-circular manifold, which is suitable for most of non-circular coat-hanger dies used in industry.

Combining the pressure drop/flow rate equations for the flows in the manifold and in the slot and the mass conservation equation in the manifold, they got the following two equations that determine the geometry of the manifold;

$$h = h_0 \left(1 - \frac{y}{L}\right)^{n/3n+1}, \quad (1)$$

$$h_0 = \left(\frac{LW^{2+(1/n)}}{\lambda N} \right)^{n/3n+1} (\csc \theta)^{1/3n+1}, \quad (2)$$

where

$$N = 2^{1+(1/n)} \left(2 + \frac{1}{n}\right). \quad (3)$$

In these equations, h is the characteristic length of the manifold, which is chosen as a square root of the cross-sectional area of the manifold, and h_0 is the value of h at die inlet. The shape factor, λ , in Eq. (2) depends on the power-law index, n and the

shape of manifold cross-section from the pressure drop/flow rate equation in the manifold. Shape factor, λ , can be approximated by the following equation [Liu, 1983].

$$\lambda(n) = \left[a^{1/n} \left(\frac{b}{n} + c \right) \right]^{-1}, \quad (4)$$

where the constants a , b , and c are functions of the cross-sectional shape of the manifold. If the equilateral triangular manifold is adopted for example, $a = 4.38$, $b = 1.04$, and $c = 6.88$. The other design parameters appearing in Eq. (1) and (2) are half the width of die L , the slot thickness W , the manifold angle θ , and the power-law index n . Under the assumption of one-dimensional flow in the manifold and the slot respectively, we can construct coat-hanger die aimed at uniform flow rate distribution using above design equations.

2. Three-dimensional Model

The flow in the coat-hanger die is three-dimensional by nature because manifold and slot section have different cross-sectional shapes. To get precise and detailed description of flow field in the die, it is necessary to analyze based on three-dimensional model. Again, the polymer melt flow is assumed to be incompressible, creeping, and isothermal. Under these assumptions, the conservation equations of mass and momentum can be written as

$$\nabla \cdot \mathbf{u} = 0, \quad (5)$$

and

$$\nabla \cdot \boldsymbol{\sigma} = 0. \quad (6)$$

As in the die design analysis, the polymer melt is assumed to be a power-law fluid. Then, the constitutive equations that relate stress tensor to deformation tensor are

$$\boldsymbol{\sigma} = -p\mathbf{I} + \mu(\nabla\mathbf{u} + \nabla\mathbf{u}^T), \quad (7)$$

where

$$\mu = K\dot{\gamma}^{n-1}. \quad (8)$$

The three-dimensional model is completed with the following boundary conditions. At the die inlet, only the axial velocity component exists and is assumed to have fully-developed velocity profile. Since the axial direction is x in Fig. 1, the governing equation for the velocity profile at die inlet can be written as

$$-\frac{\partial p}{\partial x} + \left[\frac{\partial}{\partial y} \left(\mu \frac{\partial u_x}{\partial y} \right) + \frac{\partial}{\partial z} \left(\mu \frac{\partial u_x}{\partial z} \right) \right] = 0. \quad (9)$$

Additionally, the total flow rate, that is a surface integral of the axial velocity in the die inlet plane, is set to be $150 \text{ cm}^3/\text{sec}$ in all cases. At the solid wall, no-slip condition is applied, i.e.,

$$\mathbf{u} = 0. \quad (10)$$

On the symmetry plane, the normal stress vector and the normal component of velocity vector are zero, i.e.,

$$\mathbf{n} \cdot \boldsymbol{\sigma} = 0, \quad \mathbf{n} \cdot \mathbf{u} = 0. \quad (11)$$

At the die exit, the normal component of the normal stress vector is zero and the pressure is assumed to be constant at the die exit as the reference value of zero, i.e.,

$$\mathbf{n} \cdot (\mathbf{n} \cdot \boldsymbol{\sigma}) = 0, \quad p = 0. \quad (12)$$

3. Finite Element Formulation

Table 1. Design parameters used in the simulation

Parameter	Value
W	3 cm, 4 cm, 5 cm
θ	10°, 15°, 20°, 30°
n_d	1.0, 0.5, 0.4
l_i	4 cm, 6 cm, 8 cm

Our numerical approach is to apply Galerkin/finite element method to the governing equations of the three-dimensional model. General principles of finite element method can be found in many texts such as one by Zienkiewicz [1989]. There are two finite element formulation schemes, mixed and penalty formulation, for the solution of velocity and pressure variables from Navier-Stokes equation. The mixed formulation is more rigorous and is used in this study. The coat-hanger die is discretized using three-dimensional Lagrangian element. The velocity and pressure variables are approximated by triquadratic basis function, Φ' , and discontinuous piecewise linear basis function, Ψ' , respectively. In Galerkin weighted residual formulation, the weight functions for the continuity and momentum equations are basis functions for the pressure and velocity respectively. Then the weak forms of continuity and momentum equations are

$$\iiint_V \Psi' \nabla \cdot \mathbf{u} \, dV = 0, \quad (13)$$

and

$$\iiint_V \Phi' \nabla \cdot \sigma \, dV = 0. \quad (14)$$

Application of the relation of $\nabla \cdot (\Phi' \sigma) = \nabla \Phi' \cdot \sigma + \Phi' \nabla \cdot \sigma$ and divergence theorem to Eq. (14) gives

$$\iint_{\partial V} \Phi' \sigma_n \, dA - \iiint_V \nabla \Phi' \cdot \sigma \, dV = 0. \quad (15)$$

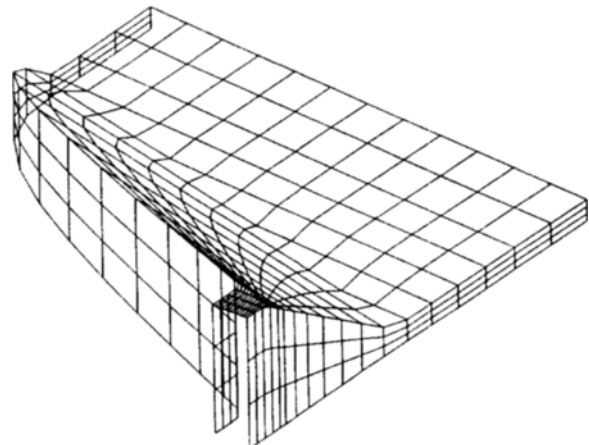
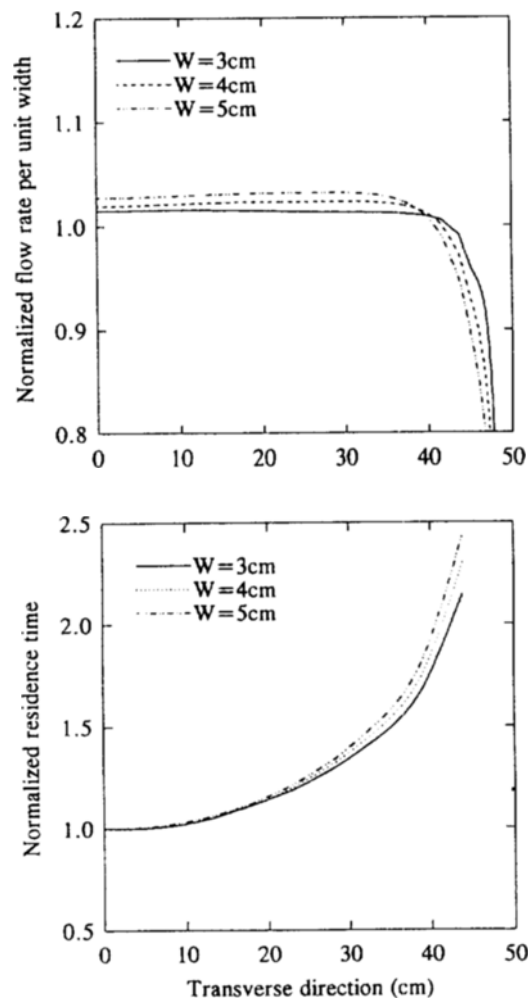
Discretization of Eqs. (13) and (15) by finite element method and integration using Gauss-Legendre quadrature give the residual equation, which is a set of nonlinear algebraic equations by the use of power-law model. The Newton-Raphson iteration scheme is then used to solve nonlinear algebraic equation set.

The set of linear equations obtained from Newton iteration has been solved using frontal algorithm developed by Hood [1976]. The number of linear equations to be solved is well over 20,000 and Hood's frontal scheme is attractive over full matrix solver in that the core memory is much less used.

In order to get flow field corresponding to the power-law index less than one, analytic continuation has been used starting from flow index of 1.0.

RESULT AND DISCUSSION

The cross-sectional shape of the manifold was modelled as equilateral triangle to simulate the real coat-hanger die used in industry. Among the design parameters determining the geometry of the coat-hanger die shown in Fig. 1, the values of half the die width L and the land length l_o have been set as 50 cm and 10 cm, respectively. Several values of other design parameters influencing on the performance of the die used in the simulation are given in Table 1, where l_i is half the width of the die inlet. Two kinds of flow indices, n_d and n_{fluid} , are used to denote a power-

**Fig. 2. Bird's-eye view of 3-dimensional mesh.****Fig. 3. Effect of slot thickness on (a) flow rate and (b) residence time distribution with $n_{fluid}=0.5$, $n_d=0.5$, $\theta=15^\circ$, and $l_i=4$ cm.**

law index for the design equation and for the fluid property, respectively. The bird's-eye view of the three-dimensional mesh used in the simulation is shown in Fig. 2. Only a quarter of a die is chosen as a domain of numerical analysis due to the symmetry of the coat-hanger die. The total number of finite element

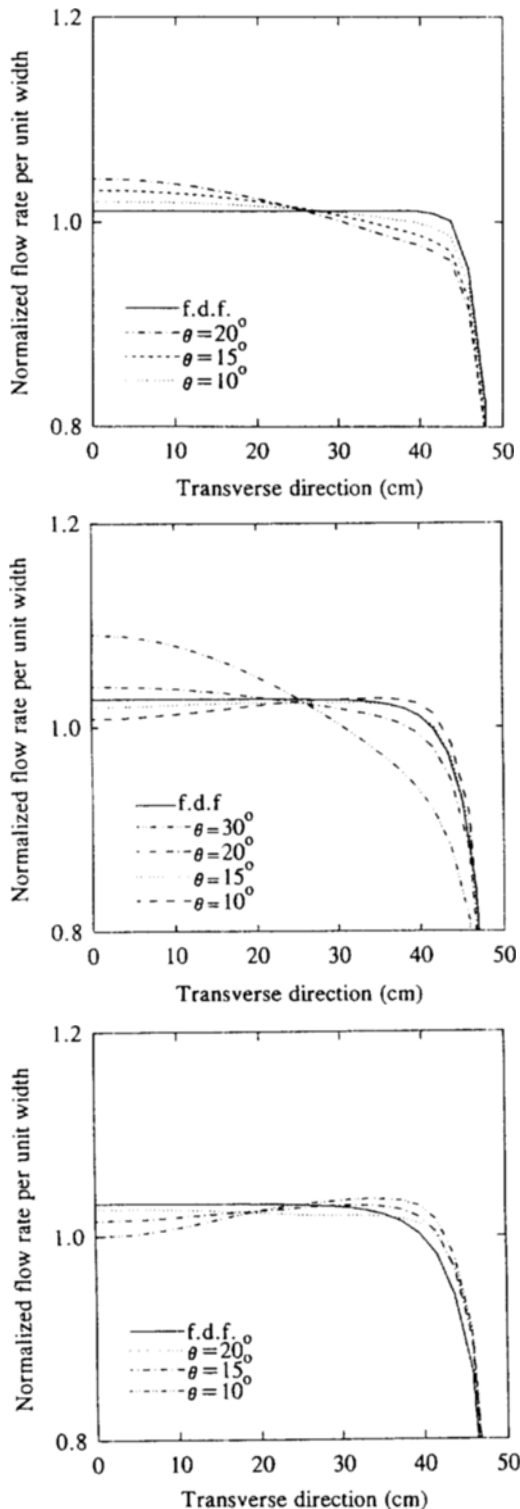


Fig. 4. Effect of manifold angle on flow rate distribution with $W=4$ cm, and $l_i=4$ cm. (a) $n_{fluid}=n_d=1.0$, (b) $n_{fluid}=n_d=0.5$, (c) $n_{fluid}=n_d=0.4$.

is 648 using 18 elements in x-direction, 12 in y-direction, and 3 in z-direction. For 648 finite elements, the total number of unknowns to be solved is 22,017 that is sum of 19,425 for velocity and 2,592 for pressure. Before applying to the die problem, computer code was tested for the case of fully-developed flow in a

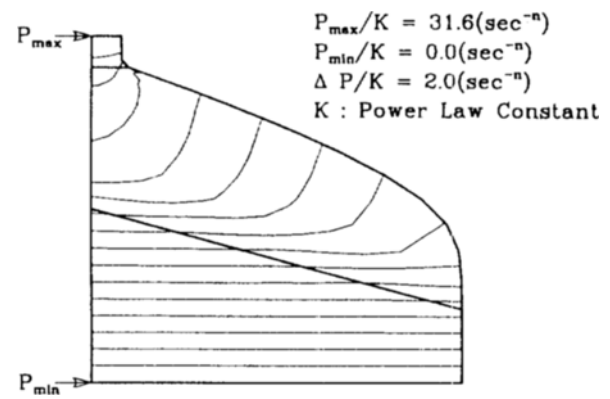


Fig. 5. Contours of pressure field with $n_{fluid}=0.5$, $n_d=0.5$, $\theta=15^\circ$, $W=4$ cm, and $l_i=4$ cm.

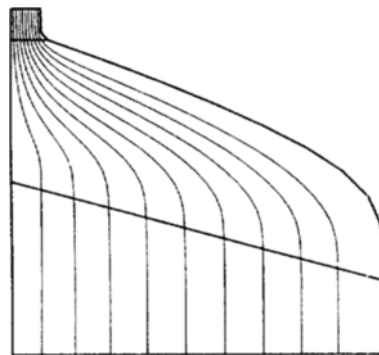


Fig. 6. Pathlines on the x-y symmetry plane with $n_{fluid}=0.5$, $n_d=0.5$, $\theta=15^\circ$, $W=4$ cm, and $l_i=4$ cm.

rectangular duct and compared with an analytical solution [White, 1974] to validate the accuracy of the code.

1. Effect of Slot Thickness

The flow rate distributions in the transverse direction have been calculated at the die exit for three different slot thickness and are shown in Fig. 3(a). The flow rate is calculated by integrating axial velocity from $z=0$ to W and normalized by the average value for comparison. In this calculation, we set $n_d=0.5$, $\theta=15^\circ$, and $l_i=4$ cm. The power-law index for fluid property n_{fluid} is 0.5 which is the same as that for the design equation n_d . As slot thickness increases, the region of uniform flow rate decreases proportional to slot thickness, as shown in Fig. 3(a). The design by one-dimensional design equation gives the uniform flow rate around the center irrespective of the slot thickness but it cannot guarantee the uniform flow rate across the entire length of exit.

The residence time distribution, shown in Fig. 3(b), was calculated along the pathlines on the x-y symmetry plane, i.e. bottom of numerical domain. Residence time in Fig. 3(b) is normalized by the value along the centerline. The residence time distributions for different slot thickness show negligible change near the center plane but they begin to deviate from each other near the side wall. Non-uniform flow rate distribution or deviation of residence time distribution near the side wall is speculated to be a result of no-slip boundary condition imposed at the side wall.

2. Effect of Manifold Angle

We next examined how the manifold angle, θ , in Fig. 1 affects the flow rate and residence time distributions. Only the manifold

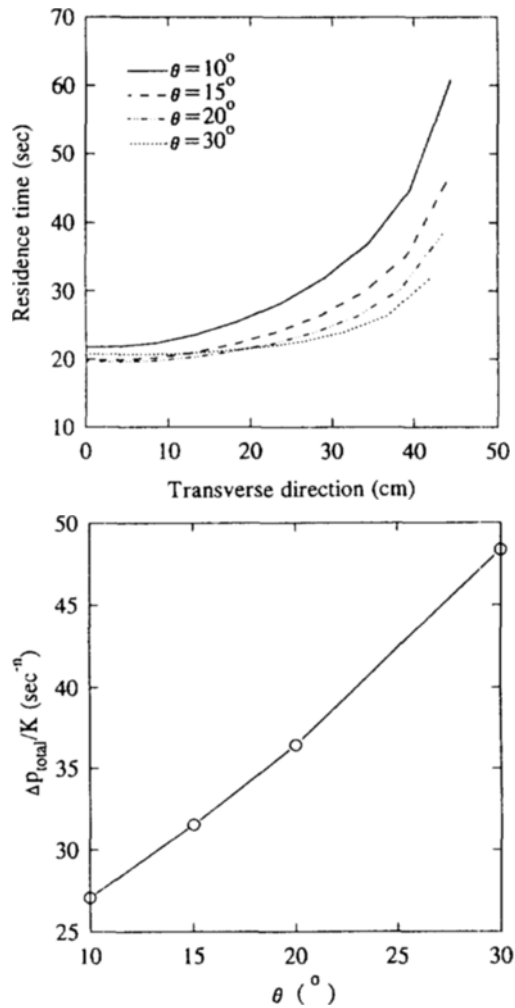


Fig. 7. Effect of manifold angle on (a) residence time distribution and (b) total pressure drop with $n_{\text{fluid}}=0.5$, $n_d=0.5$, $W=4$ cm, and $l_i=4$ cm.

angle is varied while flow indices, n_{fluid} and n_d are set to have the same value of 0.4, 0.5 or 1.0 with $W=4$ cm and $l_i=4$ cm. The flow rate distributions for several manifold angles are shown in Fig. 4(a) for $n_{\text{fluid}}=1.0$, Fig. 4(b) for $n_{\text{fluid}}=0.5$, and Fig. 4(c) for $n_{\text{fluid}}=0.4$. For comparison, the flow rate distribution for the fully developed flow (denoted as f.d.f) at the imaginary exit of sufficiently long land is shown together.

In these figures, it is shown that the flow rate distribution is very sensitive to the manifold angle. The flows are driven to the die center as the manifold angle increases in all cases. Optimum manifold angle, which maximizes the region of uniform flow rate, varies as power-law index changes. The optimum manifold angle increases from 10° to 20° as the power-law index is decreased from 1.0 to 0.4. If the manifold angle greater than the optimum value is used, flow is driven to the die center.

Pressure distribution and pathlines obtained for the most uniform flow rate distribution in Fig. 4(b), $\theta=15^\circ$, are shown in Figs. 5 and 6. Pressures shown in Fig. 5 is average values in z-direction and pathlines in Fig. 6 are calculated on the x-y symmetry plane as in Fig. 3(b). Pressure differences between isobars are uniform, so that the pressure loss can be guessed by the number of isobars between two points.

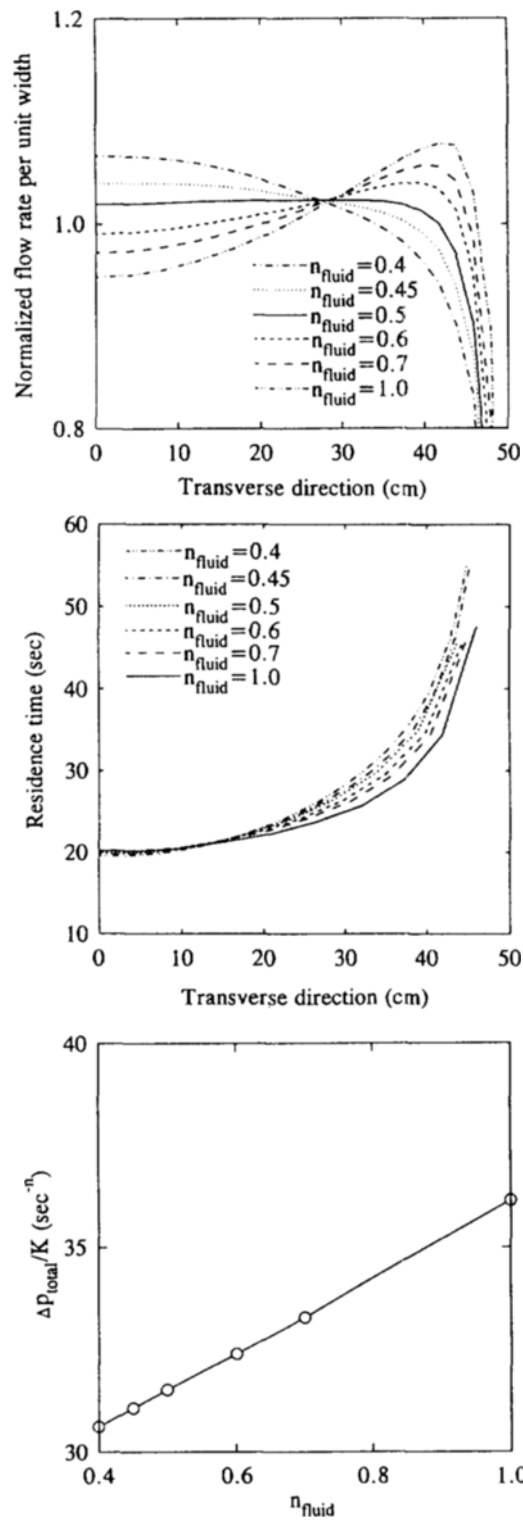


Fig. 8. Effect of n_{fluid} on (a) flow rate, (b) residence time distribution and (c) total pressure drop with $n_d=0.5$, $\theta=15^\circ$, $W=4$ cm, and $l_i=4$ cm.

Isobars in the slot section in Fig. 5 is nearly straight line parallel to y-direction, implying the pressure gradient acts only in x-direction. This agrees with assumption used to derive the one-dimensional design equation. Pathlines in Fig. 6 show that there are no irregularities such as recirculating flow or dead spots on the

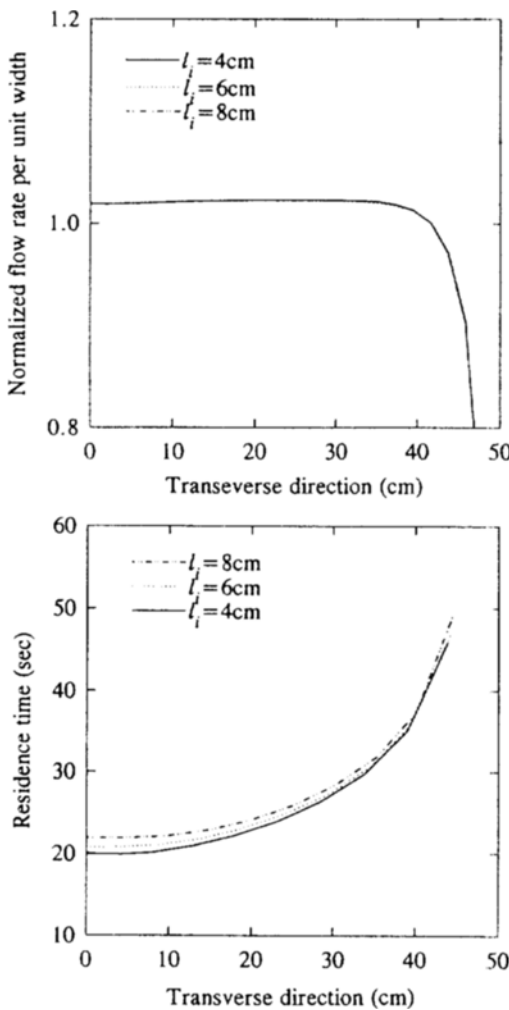


Fig. 9. Effect of l_i on (a) flow rate and (b) residence time distribution with $n_{fluid}=0.5$, $n_d=0.5$, $\theta=15^\circ$, and $W=4\text{ cm}$.

x-y symmetry plane that is detrimental to the product quality due to over heating.

Residence time distributions for $n_{fluid}=n_d=0.5$ are shown in Fig. 7(a) with varying manifold angle. The uniformity of residence time distribution improves consistently with the increase of manifold angle. However, the increase of the manifold angle is enabled with a longer die, which requires higher duty of extrusion pressure drop that is directly related to the process cost. The design equation selected in this study does not include the uniform residence time distribution as a design objective. It is known that die design results in a too long coat-hanger section if both the uniform flow rate and residence time distributions are to be satisfied at the same time [Matsubara, 1979]. Consequently, there can be a trade-off between uniform residence time distribution and the die length. To demonstrate the increased pressure drop with manifold angle, total pressure drop has been plotted in Fig. 7(b) with varying manifold angle, where $n_{fluid}=n_d=0.5$. Total pressure drop is shown to increase linearly with the manifold angle as expected.

3. Effect of Fluid Property

Flow of the polymer melt with varying power-law index is simulated in the same die to analyze the performance of die when the polymer melt processed has a different power-law index from

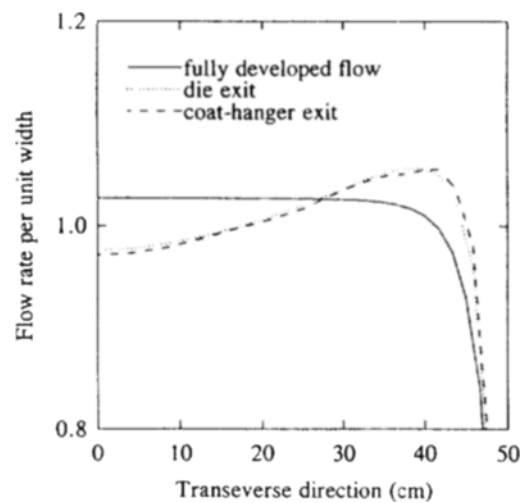


Fig. 10. Effect of land on flow rate distribution with $n_{fluid}=0.5$, $n_d=0.4$, $\theta=15^\circ$, and $W=4\text{ cm}$.

that used in the design. Die was designed according to one-dimensional design equation to result in $\theta=15^\circ$, $W=4\text{ cm}$, and $l_i=4\text{ cm}$, for the material of $n_d=0.5$. As can be seen in Fig. 8(a), the use of polymer melt which has a power-law index other than the design value can deteriorate the flow rate uniformity. Flow of fluid with smaller power-law index than the design value tends to increase near the center plane, while larger power-law index fluid flows more near side wall.

The effect of power-law index on the residence time distribution is shown in Fig. 8(b). Residence time distribution is not so sensitive to the change of power-law index as flow rate distribution. The total pressure drop in Fig. 8(c) shows linear relationship with the power-law index variation. The change of total pressure drop makes it necessary to control upstream pressure when using polymer melt with different power-law index.

4. Effect of Die Inlet

In the analytic approaches on the coat-hanger dies, the die inlet is generally considered as a point source. But the practical geometry of the die inlet is of some dimension although very small in comparison to the total die width. Here, the effect of finite die inlet is considered for the more robust analysis of the coat-hanger die by varying half the width of the die inlet, l_i , assuming rectangular cross-section. The other design parameters are set as $n_{fluid}=0.5$, $n_d=0.5$, $\theta=15^\circ$, and $W=4\text{ cm}$. The flow rate and residence time distributions with the varying l_i are shown in Fig. 9(a) and Fig. 9(b) respectively. Effect of the die inlet size on the die performance is shown to be negligible if the ratio of the die inlet size to the total die width is as small as 0.1, which is the case in industry.

5. Effect of Land

The slot section of the coat-hanger die is divided into the pre-land of triangular shape that is a part of the coat-hanger section and the land that plays as a connector between the coat-hanger section and the die exit. Practical coat-hanger dies are modified by additional devices, such as choker bars and flexible lips, in part of land to improve flow uniformity. The use of longer land will give more developed flow at the die exit.

To see the effect of the presence of land on the uniformity of flow rate, two kinds of flow rate distributions are calculated and shown in Fig. 10. One is at the coat-hanger exit where mani-

fold section ends and the other is at the die exit where land section ends. The design parameters are set as $n_{fluid}=0.4$, $n_d=0.5$, $\theta=15^\circ$, and $l_s=4$ cm. Different flow indices for design and processed material are selected to amplify the nonuniformity of flow rate. The land used in this calculation has a uniform thickness of $W=4$ cm. As shown in Fig. 10, the presence of land does not improve the uniformity of flow rate distribution. Although the infinite length of land will give the more uniform, fully-developed flow, short land with the length of one tenth of the total die width does not contribute to the uniformity of flow rate.

CONCLUSION

Flow of non-Newtonian power-law fluid in the coat-hanger die has been studied through the three-dimensional numerical simulation using finite element method. This study has been focused on the effect of design parameters on the die performance in terms of flow rate distribution and residence time distribution based on the design equation developed previously.

The slot thickness shows negligible effect on the flow rate distribution while the manifold angle is found to be the important factor for maximizing the uniformity of flow rate. Optimum manifold angle can be determined for each power-law index. The optimum manifold angle increases from 10° to 20° as the power-law index is decreased from 1.0 to 0.4. The flows tend to move to the die center when the manifold angle is greater than the optimum.

The effect of the fluid property in terms of power-law index on the performance of the coat-hanger die was investigated to provide the useful information when the process material has to be changed for a given die. Numerical results indicate that the fluid property greatly affects the flow rate distribution so that flow of fluid with smaller power-law index tends to concentrate near the die center.

With respect to the residence time distributions, there is a negligible effect of the slot thickness on the residence time distribution. The change of the power-law index does not affect the residence time distribution appreciably. The most influencing design parameter on the residence time distribution is the manifold angle. But it has also to be taken into account that the total pressure drop increases with the manifold angle, which increases the processing cost in turn.

Finally, the effect of the die inlet and the land were examined. The die inlet with the small size compared to the total die width shows negligible effect on both the flow rate and residence time distributions. The role of the land of uniform thickness in improving flow rate uniformity seems to be insignificant.

ACKNOWLEDGEMENT

Authors wish to thank to Dr. Jung Soo Yoo of Lucky R&D Center for providing viscosity data for LDPE, PMMA and ABS.

NOMENCLATURE

A	: area [cm^2]
a, b, c	: constants in Eq. (4) [-]
h	: characteristic length of the manifold [cm]
h_s	: characteristic length of the manifold at the die inlet [cm]
I	: identity matrix [-]
K	: power-law constant [$\text{g}\cdot\text{cm}^{-1}\text{sec}^{-2}$]

L	: half the die width [cm]
l_s	: half the die inlet width [cm]
l_o	: the land length [cm]
n	: power-law index [-]
n_d	: power-law index for design equation [-]
n_{fluid}	: power-law index for processed fluid [-]
n	: outward unit normal vector [-]
p	: pressure [$\text{g}\cdot\text{cm}^{-1}\text{sec}^{-2}$]
\mathbf{u}	: velocity vector [$\text{cm}\cdot\text{sec}^{-1}$]
u_x, u_y, u_z	: components of velocity vector [$\text{cm}\cdot\text{sec}^{-1}$]
V	: volume [cm^3]
W	: slot thickness [cm]
x, y, z	: global coordinates [cm]

Greek Letters

$\dot{\gamma}$: magnitude of the rate of strain tensor [sec^{-1}]
θ	: manifold angle [$^\circ$]
λ	: shape factor [-]
μ	: viscosity [$\text{g}\cdot\text{cm}^{-1}\text{sec}^{-1}$]
σ	: stress tensor [$\text{g}\cdot\text{cm}^{-1}\text{sec}^{-2}$]
Φ'	: triquadratic basis functions [-]
Ψ'	: discontinuous, piecewise linear basis functions [-]

REFERENCES

- Arpin, B., Lafleur, P. G. and Vergnes, B., "Simulation of Polymer Flow through a Coat-Hanger Die: A Comparison of Two Numerical Approaches", *Polym. Eng. Sci.*, **32**, 206 (1992).
- Booy, M. L., "A Network Flow Analysis of Extrusion Dies and Other Flow Systems", *Polym. Eng. Sci.*, **22**, 432 (1982).
- Carley, J. F., "Flow of Melts in Crosshead-Slit Dies; Criteria for Die Design", *J. Appl. Phys.*, **25**, 1118 (1954).
- Carley, J. F., "Design and Operation of Crosshead Sheeting Dies", *Mod. Plast.*, **33**, 127 (1956).
- Fortin, M., "Old and New Finite Elements for Incompressible Flows", *Int. J. Num. Meth. Fluids*, **1**, 347 (1981).
- Gutfinger, C., Broyer, E. and Tadmor, Z., "Analysis of a Cross Head Die with the Flow Analysis Network (FAN) Method", *Polym. Eng. Sci.*, **15**, 383 (1975).
- Hood, P., "Frontal Solution Program for Unsymmetric Matrices", *Int. J. Num. Meth. Eng.*, **10**, 379 (1976).
- Huang, C.-C., Tsay, S.-Y. and Wang, Y., "Three-Dimensional Path Line Tracking and Residence Time Distribution in Fishtail Dies", *Polym. Eng. Sci.*, **33**, 709 (1993).
- Klein, I. and Klein, R., "Computer Modeling of Coat Hanger Dies May be Cheaper for the Long Run", *SPE J.*, **29**, 33 (1973).
- Lee, K.-Y. and Liu, T.-J., "Design and Analysis of a Dual-Cavity Coat-Hanger Die", *Polym. Eng. Sci.*, **29**, 1066 (1989).
- Liu, T.-J., "Fully Developed Flow of Power-Law Fluids in Ducts", *Ind. Eng. Chem. Fundam.*, **22**, 183 (1983).
- Liu, T.-J., Hong, C.-N. and Chen, K.-C., "Computer-Aided Analysis of a Linearly Tapered Coat-Hanger Die", *Polym. Eng. Sci.*, **28**, 1517 (1988).
- Matsubara, Y., "Geometry Design of a Coat-Hanger Die with Uniform Flow Rate and Residence Time Across the Die Width", *Polym. Eng. Sci.*, **19**, 169 (1979).
- Matsubara, Y., "Residence Time Distribution of Polymer Melt in the T-Die", *Polym. Eng. Sci.*, **20**, 212 (1980a).
- Matsubara, Y., "Design of Coat-Hanger Sheeting Dies Based on Ratio of Residence Times in Manifold and Slot", *Polym. Eng. Sci.*, **20**, 716 (1980b).

Matsubara, Y., "Residence Time Distribution of Polymer Melts in the Linearly Tapered Coat-Hanger Die", *Polym. Eng. Sci.*, **23**, 17 (1983).

McKelvey, J.-M. and Ito, K., "Uniformity of Flow from Sheet Dies", *Polym. Eng. Sci.*, **11**, 258 (1971).

Pearson, J. R. A., "Non-Newtonian Flow and Die Design: Part IV. Flat-Film Die Design", *Trans. J. Plastics Inst.*, **32**, 239 (1964).

Procter, B., "Flow Analysis in Extrusion Dies", *SPE J.*, **28**, 34 (1972).

Tadmor, Z., Broyer, E. and Gutfinger, C., "Flow Analysis Network (FAN)-A Method for Solving Flow Problems in Polymer Processing", *Polym. Eng. Sci.*, **14**, 660 (1974).

Tadmor, Z. and Gogos, C. G.: "Principles of Polymer Processing", John Wiley, New York, 1979.

Vergnes, B., Saillard, P. and Agassant, J. F., "Non-Isothermal Flow of a Molten Polymer in a Coat-Hanger Die", *Polym. Eng. Sci.*, **24**, 980 (1984).

Vrahopoulou, E. P., "A Model for Fluid Flow in Dies", *Chem. Eng. Sci.*, **46**, 629 (1991).

Wang, Y., "The Flow Distribution of Molten Polymers in Slit Dies and Coathanger Dies through Three-Dimensional Finite Element Analysis", *Polym. Eng. Sci.*, **31**, 204 (1991a).

Wang, Y., "Extrusion of Rubber Compounds and Highly Filled Thermoplastics through Coathanger Dies", *Int. Polym. Proc.*, **6**, 311 (1991b).

White, F. M., "Viscous Fluid Flow", McGraw-Hill, New York, 1974.

Winter, H. H. and Fritz, H. G., "Design of Dies for the Extrusion of Sheets and Annular Parisons: The Distribution Problem", *Polym. Eng. Sci.*, **26**, 543 (1986).

Zienkiewicz, O. C. and Taylor, R. L., "The Finite Element Method", 4th ed., McGraw-Hill, London, 1989.